Piezo2 mediates cannabidiol-induced analgesia of mechanical allodynia

Qijing He[1,2,3,4,5,*], Ruijia Lai[6,7*], Wanru Huang[1,2,3,4,5,*], Hongyuan Zuo[1,2,3,4,5*], Kun Cao[6], Mengya Cai[7], Feng Qian[1], Yang Zhang[6,7,#], Bailong Xiao[1,2,3,4,5,#]

[1]State Key Laboratory of Membrane Biology, School of Pharmaceutical Sciences, Tsinghua Medicine, Tsinghua University, Beijing, 100084, China;
[2]New Cornerstone Science Laboratory, School of Pharmaceutical Sciences, Tsinghua Medicine, Tsinghua University, Beijing, 100084, China;
[3]Tsinghua-Peking Center for Life Sciences, Tsinghua University, Beijing, 100084, China;
[4]IDG/McGovern Institute for Brain Research, Tsinghua University, Beijing, 100084, China.
[5]Beijing Frontier Research Center of Biological Structure, Tsinghua University, Beijing, 100084, China;
[6]Institute of Molecular Physiology, Shenzhen Bay Laboratory, Shenzhen, China
[7]Shenzhen Medical Academy of Research and Translation, Shenzhen, China

[*]These authors contribute equally to this work.
[#]To whom correspondence should be addressed:
zhangyang@szbl.ac.cn, Tel: (+86) 17771318306
xbailong@mail.tsinghua.edu.cn, Tel.: +86-10-62773981

Abstract

Cannabidiol (CBD), a clinically approved but non-psychoactive component of cannabis, has demonstrated analgesic effects in both human and rodent models of chronic pain[1-6]. However, the molecular mechanisms underlying CBD's analgesic properties, particularly in mechanical allodynia, remain unclear. The mechanically activated ion channel Piezo2 is a genetically validated mechanoreceptor for touch and mechanical allodynia in both humans and mice[7-11]. Here, we show that both systemic (intraperitoneal) and local (intraplantar) administration of CBD into wild-type mice specifically suppress behavioral responses to gentle touch and mechanical allodynia in pain models, without affecting responses to noxious heat or heat hyperalgesia. Importantly, the specific effects on touch and mechanical allodynia are abolished in Piezo2-deficient mice. Mechanistically, CBD inhibits Piezo2-mediated mechanically activated and rapidly adapting currents in primary sensory neurons and in heterologous cells expressing mouse Piezo2. CBD directly binds to purified Piezo2 proteins with measurable affinity. Additionally, CBD inhibits human PIEZO2-mediated mechanically evoked currents. These findings identify Piezo2 as a long-sought-after receptor mediating CBD's analgesic effects in mechanical allodynia, validate Piezo2 as a promising non-opioid analgesic target, and provide a mechanistic foundation for developing CBD-derived pain therapies.

Keywords

Cannabidiol (CBD), Piezo2, Piezo1, mechanical allodynia, chronic pain, non-opioid analgesics, cannabis, tetrahydrocannabinol

Main

Cannabidiol (CBD) is a non-psychoactive compound derived from the cannabis plant that has attracted considerable attention for its therapeutic potential. In addition to its clinical approval for treating certain forms of epilepsy[12,13], both preclinical and clinical studies have demonstrated that CBD exerts analgesic effects in a wide range of pain conditions, including inflammatory and neuropathic pain[1-6,14,15]. Unlike the primary psychoactive component of cannabis tetrahydrocannabinol (THC) or opioid analgesics, which carry substantial risks of addiction and adverse effects, CBD offers a promising alternative due to its favorable safety profile and lack of psychoactive properties.

Despite its therapeutic potential as a non-opioid analgesic, the molecular mechanisms underlying CBD's analgesic actions particularly in mechanical allodynia remain unclear. In contrast to THC, which primarily exerts its effects through cannabinoid receptors CB1 and CB2, CBD exhibits low affinity for these canonical receptors[16-18]. Moreover, pharmacological blockade of CB1/CB2 fails to reverse CBD's antihyperalgesic effects[19]. Previous studies have shown that CBD can activate multiple transient receptor potential (TRP) channels expressed in primary sensory neurons of dorsal root ganglion (DRG)[20-23], including TRPV1, TRPV2, and TRPA1, which are key mediators of nociceptive responses to noxious heat and chemical stimuli[24]. However, activation of these nociceptive channels appears paradoxical to CBD's analgesic

actions. In line with this, some studies reported that CBD has limited effects in blocking heat nociception and hyperalgesia, but exhibits more robust efficacy in suppressing mechanical allodynia[5,25-27].

Piezo2, a mechanically activated ion channel expressed in primary sensory neurons, plays a central role in converting mechanical stimuli into electrical signals[7,28-30]. Genetic studies in both mice and humans have demonstrated that Piezo2 mediates the sensation of light touch and mechanical allodynia under inflammatory and neuropathic conditions[8-11,31], in which normally innocuous stimuli are perceived as painful. Piezo2 has also been implicated in visceral pain and osteoarthritic joint pain[32-34]. Despite growing recognition of its importance in mechanical pain, the pharmacological targeting of Piezo2 remains challenging due to the lack of selective and clinically viable inhibitors. Existing blockers, such as the peptide GsMTx4 and broad cation channel inhibitors like ruthenium red[7,35], exhibit substantial off-target effects, including inhibition of the closely related Piezo1 channel[7,36], limiting their therapeutic utility.

Given the critical role of Piezo2 in mechanical allodynia, we investigated whether CBD directly interacts with and modulates Piezo2 function in vivo and in vitro. Our findings demonstrate that CBD potently inhibits Piezo2-mediated currents, thereby suppressing touch sensation and mechanical allodynia in pain models.

CBD selectively suppresses mechanical allodynia in various pain models

We first behaviorally examined whether CBD might effectively inhibit Piezo2-mediated gentle touch in naïve mice and mechanical allodynia in mice with complete Freund's adjuvant (CFA)-induced inflammation using von Frey filaments. A hot plate test was also conducted to assay the effect of CBD on heat nociception and hyperalgesia. Different doses of CBD were delivered either systemically via intraperitoneal injection or locally via intraplantar injection to assay its specific effects at the primary sensory transduction site.

Compared with the vehicle-treated group of naïve mice, systemic administration of CBD at doses of 1 mg/kg and 10 mg/kg reduced paw withdrawal responses to Von Frey filaments with forces below 0.6 g, but had no apparent blocking effect on Von Frey filaments with high forces of 2g and 4g (Figure 1a). Similar inhibitory effect was observed with intraplantar injection of CBD at 2 mM, but less effective at 0.5 mM and 1 mM (Figure 1e), demonstrating a dose-dependent inhibitory effect. These data suggest that both systemically and locally applied CBD inhibits gentle touch sensation in naïve mice, which resembles the previously observed touch deficit phenotype in mice with Piezo2 deletion in DRG sensory neurons[8,37].

Mice with CFA-induced inflammation showed increased paw withdrawal responses to Von Frey filaments with low forces ranging from 0.04 g to 0.6 g, demonstrating inflammation-induced mechanical allodynia (Figure 1c,g). Remarkably, systemically applied CBD at both 1 mg/kg and 10 mg/kg caused a robust inhibition of the response

of mechanical allodynia, but had no effect on the responses elicited by Von Frey filaments with high forces of 2 g (Figure 1c). Local administration of 1 mM or 2 mM CBD also attenuated the CFA-induced mechanical allodynia albeit with a relatively weaker effect than systemically applied CBD (Figure 1g).

In contrast to the apparent inhibitory effect of CBD on touch and mechanical allodynia, we found that neither systemic nor local CBD administration at the tested doses significantly affected heat nociception in naïve mice or heat hyperalgesia in CFA-induced inflammatory mice (Figure 1b, d, f, h), which is consistent with previous reports[26,27,38,39], but contradicts the observed anti-heat nociception by the use of 30 mg/kg of CBD in rats[40]. Collectively, these data indicate that CBD strongly inhibits Piezo2-mediated touch and CFA-induced allodynia, without affecting Piezo2-independent thermal perception.

We further assessed the efficacy of CBD on mechanical allodynia and hyperalgesia in complementary mouse models that capture acute inflammatory and chronic neuropathic pain states. Mechanical sensitivity was quantified using a standardized battery of behavioral assays, including von Frey filaments, pinprick, and light brushing stimulation. We first examined CBD in the capsaicin-induced acute inflammation model[22], which recapitulates key features of nociceptive sensitization. Capsaicin injection produced a pronounced and sustained reduction in mechanical withdrawal thresholds to von Frey stimulation over the 1-h testing period and elicited robust nocifensive behaviors in response to pinprick and brush stimuli applied to the plantar hindpaw. Although CBD-treated mice exhibited a similar initial drop in von Frey threshold at 15 min, their responses progressively recovered thereafter, in sharp contrast to the persistent hypersensitivity observed in vehicle controls (Extended Data Figure 1a). CBD likewise attenuated pinprick-evoked nociceptive and brush-evoked allodynia responses (Extended Data Figure 1b,c). Together, these findings indicate that CBD effectively counteracts capsaicin-evoked mechanical allodynia.

To evaluate the effect of CBD in chronic neuropathic pain, we employed the spared nerve injury (SNI) model, which produces robust and persistent mechanical allodynia by postoperative day 7. As expected, SNI mice exhibited marked reductions in von Frey mechanical withdrawal thresholds compared with sham controls (Extended Data Figure 1d). Administration of CBD on day 7 post-injury elicited a rapid increase in mechanical thresholds within 15 minutes, with sensitivities progressively recovering to levels nearly indistinguishable from sham mice (Extended Data Figure 1d). Furthermore, CBD significantly attenuated both pinprick-evoked punctate hyperalgesia and brush-induced dynamic allodynia (Extended Data Figure 1e,f), suggesting that CBD effectively reverses the mechanical hyperalgesia and allodynia associated with peripheral nerve injury.

Collectively, these data demonstrate that CBD selectively inhibits gentle touch and confers potent anti-allodynic efficacy across acute, inflammatory, and neuropathic pain

states. These findings highlight the potential of CBD as a broad-spectrum therapeutic candidate for the management of mechanical pain hypersensitivity associated with inflammatory and neuropathic conditions.

CBD inhibition of mechanical sensitivity is mediated by Piezo2

We next investigated whether the suppressive effects of CBD on tactile sensation and inflammatory mechanical allodynia are Piezo2-dependent. Global knockout of Piezo2 in mice results in perinatal lethality[8]. Thus, we employed an established strategy to functionally ablate Piezo2 in sensory neurons by delivering adeno-associated virus (AAV) encoding Piezo2-targting sgRNA (sgPiezo2) to neonatal CRISPR-Cas9 mice[41]. Using this approach, we successfully generated control and sgPiezo2-targeted mice. Consistent with mice with Advillin-Cre-induced deletion of Piezo2 in sensory DRG neurons[8], sgPiezo2-targeted mice showed markedly impaired responses to low forces of Von Frey filaments under both normal or inflammatory conditions, but unchanged responses to noxious heat and heat hyperalgesia (Figure 2). These data demonstrate specific impaired sensation of gentle touch and mechanical allodynia in the sgPiezo2-targeted mice.

Based on our established effective dose of CBD on inhibiting the touch and mechanical allodynia (Figure 1), we tested 10 mg/kg CBD systemically and 2 mM CBD locally. In control mice, systemic CBD administration significantly reduced paw withdrawal responses to von Frey filaments in both naïve and CFA-induced inflammatory pain model (Figure 2a,c). By contrast, CBD had no further inhibitory effect in sgPiezo2-targeted mice (Figure 2a,c). Meanwhile, noxious heat sensitivity and inflammation-induced heat hyperalgesia were unchanged by CBD in either control or sgPiezo2-targeted mice (Figure 2b,d).

To demonstrate that CBD might directly act at the primary sensory transduction site instead of indirectly acting on the central nervous system to suppress the sensation of touch and mechanical allodynia, we also performed local CBD administration. Consistently, 1 mM CBD effectively suppressed tactile responses and CFA-induced mechanical allodynia in control mice (Figure 2e,g). Importantly, locally applied CBD had no further inhibitory effect in sgPiezo2-targeted animals (Figure 2e,g). Consistent with the effect of systematic CBD, local CBD did not affect heat nociception and hyperalgesia in either genotype under normal or inflammatory conditions (Figure 2f,h). Taken together, these data demonstrate that the CBD-mediated suppression of gentle touch and pathological mechanical allodynia is mediated by Piezo2.

CBD selectively silences rapidly adapting mechanoreceptors

To determine whether the inhibitory effect of CBD on Piezo2-dependent touch and mechanical allodynia might be due to its inhibition of Piezo2-mediated mechanotransduction in DRG neurons, we examined the effect of CBD on Piezo2-mediated mechanically activated currents. Whole-cell recordings from dissociated mouse DRG neurons revealed three canonical mechanically activated current subtypes,

classified by inactivation time-constant (τ_d): rapidly adapting (RA, τ_d < 10 ms), intermediately adapting (IA,10 ms ≤ τ_d ≤ 30 ms), and slowly adapting (SA, τ_d > 30 ms) (Figure 3a)[7]. Piezo2 has been shown to mediate the RA currents in mouse DRG neurons[7,8]. Application of CBD to mouse DRG neurons produced a robust and highly selective suppression of the RA subtype, the defining electrophysiological signature of Piezo2. Following CBD treatment, the proportion of RA-responsive neurons declined markedly, while the fraction of mechanically non-responsive neurons increased from 16.8% in controls to 51.2% in treated cells (Figure 3a,b). By contrast, the incidence of IA and SA currents remained unchanged (Figure 3a,b). Among the remaining RA-responsive neurons, CBD significantly reduced peak current amplitudes and elevated mechanical activation thresholds (Figure 3c,d). By contrast, both the current amplitude and mechanical activation threshold of IA and SA were not altered by CBD (Figure 3c,d). The specific inhibitory effect of CBD on RA currents is reminiscent of those observed in Piezo2-deficient DRG neurons[7,8]. Together, these findings demonstrate that CBD inhibits Piezo2-mediated mechanically activated currents in mouse DRG neurons, which is manifested to the inhibition of behavioural responses of touch and mechanical allodynia.

CBD preferentially inhibits mPiezo2 over mPiezo1

To more directly investigate the effect of CBD on mPiezo2, we overexpressed the commonly used splicing variant 2 of mPiezo2 in the Piezo1-KO-HEK293T cells, in which the endogenous Piezo1 was knocked out. Following the application of increasing concentrations of CBD (ranging from 0.1 to 100 μM), we assessed channel activity using the standard Piezo-driven mechanical poking assay. CBD application resulted in a marked and reversible inhibition of mPiezo2-mediated currents without apparently affecting the inactivation kinetics (Figure 4a-c and Extended Data Figure 2a, b). Quantification revealed that CBD suppressed mPiezo2 currents in a concentration-dependent manner, with a calculated half-maximal inhibitory concentration (IC_{50}) of ~1.0 μM (Figure 4b,d). At higher concentrations, a subset of cells failed to generate detectable inward currents upon mechanical stimulation, precluding the fitting of inactivation kinetics and indicating near-complete channel blockade (Figure 4a,c). Comparison of current amplitudes evoked by identical stimulation depths further showed that 10 μM CBD substantially reduced currents relative to control conditions (Figure 4e).

We next examined the effect of CBD on mPiezo1, the homologue of mPiezo2. Notably, despite that high concentrations of CBD blocked mPiezo1-mediated mechanically activated whole-cell currents, the calculated IC_{50} of mPiezo1 inhibition is about 33.3 μM (Figure 4f-j). These data demonstrate that CBD more potently inhibits mPiezo2 than mPiezo1, showing a ~33-fold difference in inhibition. Notably, studies from our group and others have shown that CBD also exerts an inhibitory effect on human PIEZO1[42,43].

To exclude the possibility that the inhibitory effect of CBD on mPiezo1/2 current might be due to indirect action on CBR1/2 signaling pathways, we tested the effect of endogenous agonists of CRB1/2, including anandamide (AEA) and 2-arachidonoylglycerol (2-AG) on mPiezo1/2 current. Application of 100 μM of AEA or 2-AG neither changed the current amplitude nor the inactivation kinetics of mPiezo1- or mPiezo2-mediated currents (Extended Data Figure 3a-f). These data indicate that CBD might directly act on mPiezo1/2 instead of indirect signal transduction pathways.

Structural specificity of cannabinoid inhibition of mPiezo2

To dissect whether CBD-mediated inhibition of mPiezo2 might reflect a defined ligand-receptor interaction rather than a generic perturbation of membrane mechanics, we performed a targeted structure-activity relationship (SAR) analysis. A panel of structurally related cannabinoids was evaluated using whole-cell recordings of mPiezo2. The SAR screen revealed marked structural specificity for mPiezo2 inhibition. CBD, along with cannabigerol (CBG) and cannabinol (CBN), robustly suppressed mechanically activated mPiezo2 currents (Extended Data Figure 4a, b). By contrast, O-1918 and abnormal cannabidiol (abn-CBD), which differ in the resorcinol core or the specific pentyl side chain, produced negligible inhibition despite their comparable lipophilicity (Extended Data Figure 4a, b). Together, these findings support a model in which select cannabinoids inhibit mPiezo2 through a structure-dependent manner. The requirement for specific chemical features, combined with rapid reversibility and lack of effect from related analogs, points to a highly selective modulatory interaction rather than a nonspecific membrane-mediated effect.

CBD inhibits hPIEZO2

Given that CBD has reported analgesic effects in humans, we examined its effect on the commonly used variant 2 of human PIEZO2 (hPIEZO2), which lacks the regions encoded by exons 18, 19, 35 and 40 and preferentially responds to poking stimulation but poorly to stretch stimulation. Similar to the variant 2 of mPiezo2 (Figure 4a-e), CBD dose-dependently suppressed the mechanically activated whole-cell current mediated by hPIEZO2-variant 2, without affecting the inactivation kinetics (Figure 5a-e). However, the calculated IC_{50} of 12.9 μM is higher than that of mPiezo2 (Figure 5d), demonstrating species-dependent differences in CBD sensitivity between mPiezo2 and hPIEZO2.

CBD binds to mPiezo2 proteins

To directly test whether CBD directly binds to mPiezo2 proteins, we purified mPiezo2 proteins (Figure 6a) and conducted Bio-Layer Interferometry (BLI), which is a label-free, real-time optical technique that measures biomolecular interactions. In line with our hypothesis, we observed dose-dependent binding of CBD with mPiezo2 proteins (Figure 6b). The measured dissociation constant (K_d) for mPiezo2 is 128.5 μM (Figure 6c). Notably, the K_d value of CBD for mPiezo2 is higher than its IC_{50}. Such difference could be derived from the different measurement conditions as the BLI was conducted at 15℃ in purified mPiezo2 proteins without lipid membranes, while the

electrophysiologic recording was conducted at room temperature in living cells expressing mPiezo2. Furthermore, given its highly lipophilic nature, CBD likely partitions and accumulates within the plasma membrane of living cells. Consequently, the local effective concentration of CBD in the vicinity of the channel may significantly exceed its nominal concentration in the solution, which accounts for the lower apparent IC_{50} observed in our electrophysiological recordings. Alternatively, the binding of CBD with mPiezo2 might induce an allosteric inhibition of the channel. Regardless of the exact mechanism, these data demonstrate that CBD directly binds to mPiezo2 and consequently inhibits its channel activities.

Discussion

Cannabidiol (CBD) exhibits well-established analgesic properties, yet the molecular basis for its selective efficacy in mechanical pain has remained unclear. Here, we identify the mechanically activated ion channel Piezo2 as a direct and functionally essential target of CBD. CBD selectively suppresses gentle touch and mechanical allodynia across inflammatory and neuropathic pain models without affecting thermal nociception. These behavioral effects require Piezo2 and are accompanied by selective inhibition of Piezo2-mediated mechanically activated currents in DRG neurons, establishing a direct mechanistic link between CBD and Piezo2-mediated sense of touch and mechanical allodynia.

This finding resolves a longstanding paradox in cannabinoid pharmacology. Although CBD modulates diverse molecular targets, including activation of TRPV1, TRPV2 and TRPA1 channels in DRG neurons[20-23], these pathways do not explain its preferential efficacy in mechanical pain. By contrast, Piezo2 is the principal mechanotransducer for light touch and mechanical allodynia[8-11]. CBD directly binds Piezo2 and reduces channel open probability, consistent with allosteric gating modulation rather than pore blockade. CBD shows substantially greater potency toward Piezo2 than Piezo1, supporting the feasibility of selectively targeting peripheral mechanotransduction while minimizing systemic effects.

Importantly, species differences in CBD sensitivity between mouse Piezo2 and human PIEZO2 indicate that further optimization may be required to achieve maximal clinical efficacy. The higher IC_{50} observed for human PIEZO2 suggests potential opportunities for medicinal chemistry efforts aimed at enhancing potency, selectivity, and pharmacokinetic properties. The identification of cannabinoid structural determinants that govern Piezo2 inhibition will provide a valuable starting point for such optimization.

Together, our findings identify Piezo2 as a direct molecular target of CBD and establish selective inhibition of mechanotransduction as a central mechanism underlying its analgesic effects. These results position Piezo2 as a compelling therapeutic target and provide a framework for developing next-generation non-opioid analgesics. However, given that CBD also has inhibitory effect on Piezo1[42,43], future studies of the structural basis of CBD binding to Piezo2 will resolve the inhibitory mechanism and guide

rational design of CBD-derived pain therapies more preferentially targeting Piezo2 over Piezo1.

Materials and Methods

Animals

All experiments were conducted with the approval and support of the Animal Management Center at either Tsinghua University or Shenzhen Bay Laboratory. All mice were housed under specific pathogen-free (SPF) conditions with a 12-hour light/dark cycle and provided ad libitum access to standard chow and water. CRISPR/Cas9-mediated knockout was performed as described in the preprint[41]. Briefly, neonatal (postnatal day 0–2, P0–P2) ROSA26-Cas9-knockin mice (cyagen, China, Stock Number: C001218) received stereotaxic intracerebroventricular injections. Surgical tools (27G needles, 10 µL Hamilton syringes) were sterilized with 70% ethanol. Cryoanesthesia was induced by placing pups on crushed ice for 3–4 min, with anesthetic depth confirmed by loss of toe-pinch reflex. Stereotaxic coordinates (0.7-1.0 mm lateral to sagittal suture, 0.7-1.0 mm caudal to bregma) were marked with sterile surgical ink. *Piezo2*-targeting gRNAs were cloned into a pAV vector (WZbio, China). The following sequences were used: (1) CTTACCTTGCATCGTTGCTT; (2) TCATTGCAAGTCTGACCATC; (3) CTTACCTTGCAGGCTCAACA; (4) GCAATGAACATCCCGATATC; (5) CAATCACAGCATGTGCGTTC. AAV9 particles expressing the sgRNAs (5×10^{12} vg/mL; WZbio, China) were prepared, and 1.5 µL of the viral suspension was injected over 60 s at a depth of 2 mm using a microprocessor-controlled microinjection system. The needle was held in place for 20 s post-injection to minimize cerebrospinal fluid reflux. Pups recovered on a 37 °C warming pad before being returned to the home cage.

CFA model

Inflammatory pain was induced by subcutaneous injection of 10 µL of 50% Complete Freund's Adjuvant (CFA; MCE, Cat# 9007-81-2; diluted 1:1 in saline) into the plantar surface of the left hind paw. The 50% concentration was selected to minimize excessive inflammation. Control animals were injected with an equivalent volume of saline.

Capsaicin-mediated hypersensitivity

Capsaicin (Absin, Cat# abs817025) was initially prepared as a stock solution at a concentration of 0.1 g/ml (100 mg/ml) in 100% ethanol. For administration, this stock solution was diluted 1:1000 in a vehicle consisting of phosphate-buffered saline (PBS), 0.5% Tween 80, and 10% ethanol. A 10 µL volume of this solution was administered by intraplantar injection. Following injection, mice exhibited nociceptive behaviors, including spontaneous paw licking. Mechanical sensitivity was assessed at baseline (before injection) and at −30, 0, 15, 30, 45, and 60 min after injection of the indicated compound.

Spared Nerve Injury (SNI) Model

The spared nerve injury (SNI) model was performed as previously described [44]. Adult male C57BL/6J mice (8–10 weeks) were anesthetized with isoflurane (4% induction, 2% maintenance in oxygen). Under aseptic conditions, an incision was made in the lateral left thigh to expose the sciatic nerve and its three terminal branches: the sural,

common peroneal, and tibial nerves. The common peroneal and tibial nerves were tightly ligated with 6-0 silk suture and transected distal to the ligation, removing a 2–4 mm segment of each. Great care was taken to preserve the sural nerve intact without contact or stretching. Sham-operated mice underwent the same exposure procedure without nerve ligation or transection. Muscle layers were sutured with 6-0 absorbable suture, and skin was closed with wound clips. Mice were kept on a heating pad until ambulatory and housed individually for at least 7 days before testing. All procedures were approved by the Laboratory Animal Welfare Ethics Committee of Shenzhen Bay Laboratory (Resolution No. AEZYANG202301).

CBD injection

Cannabidiol (CBD; zzstandard, Cat# 13956-29-1) was dissolved in 75% ethanol to prepare a 20 mM stock solution. Mice received an intraperitoneal (i.p.) injection of 1/10/20 mg/kg CBD or intraplantar injection of 0.5, 1, 2 mM CBD using a microsyringe. Control groups received an equivalent volume of 75% ethanol vehicle. For the capsaicin, CBD was administered 30 min prior to the injection of the inflammatory agent. For the SNI model and CFA models, CBD was injected immediately after baseline threshold measurements.

Von Frey filament test

Male mice (8–16 weeks old) were acclimated in transparent plexiglass chambers (Ugo Basile 46000) placed on an elevated wire grid (5 mm mesh) for 30 min per day on two consecutive days. Mechanical hypersensitivity was assessed using a graded series of von Frey filaments (0.008–2.0 g; Bioseb BIO-VF-M) applied perpendicularly through the mesh to the plantar surface of the hind paw. Each filament was tested six times with 30-s intervals following the up-down method. The paw withdrawal frequency (%) was calculated as (number of positive responses/6 trials) × 100. Throughout testing, the experimenter was blinded to the genotype of the mice.

Hot plate test

Mice were placed on a 50.0 ± 0.2°C aluminum plate (Bioseb BIO-HP-LE) enclosed by a clear acrylic cylinder (20 cm diameter). Latency of hind paw licking was recorded with 60 s cutoff.

Pinprick Test

Mice were placed individually in transparent Plexiglas chambers on an elevated wire mesh grid and allowed to habituate for 30 min. A 26-gauge sterile hypodermic needle was used to apply a punctate mechanical stimulus to the plantar surface of the hind paw. The needle was applied with sufficient force to indent the skin without penetration and maintained for ~2 s. Rapid paw withdrawal, shaking, or licking was recorded as a positive response. Each paw was tested five times with an inter-stimulus interval of at least 5 min to prevent sensitization. The response frequency was calculated as the percentage of positive responses.

Cotton Swab Test

Mice were placed in individual transparent Plexiglas chambers on an elevated wire mesh grid and allowed to habituate for 30 min. A commercially available cotton-tipped applicator was used to apply a light, non-noxious stroking stimulus to the plantar surface of the hind paw. The stimulus was applied with consistent, gentle pressure in a

proximal-to-distal direction. Rapid paw withdrawal, flinching, or licking was recorded as a positive response. Each paw was subjected to five trials with an inter-trial interval of at least 5 min. Data are expressed as the percentage of positive responses.

DRG primary neurons culture

Dorsal root ganglion (DRG) neurons were isolated using an established protocol [45]. Briefly, adult male C57BL/6J mice (8–10 weeks) were anesthetized with isoflurane (4% induction, 2% maintenance in oxygen). Dorsal root ganglia (DRG) were harvested from all spinal levels following laminectomy and placed in ice-cold HBSS. Ganglia were cleaned of connective tissue and enzymatically digested in HBSS containing 3 mg/mL collagenase type II (Worthington, Cat# LS004174) and 5 mg/mL dispase (Yeasen, Cat# 40104ES60) for 30 min at 37 °C, followed by mechanical trituration. Cells were pelleted by centrifugation (160 × g, 5 min) and resuspended in 200 µL pre-warmed DMEM/F12 medium supplemented with 10% FBS and 1% penicillin-streptomycin. Cells were plated onto poly-L-lysine (Beyotime, Cat# C0312) and laminin (Macklin, Cat# L873904) coated glass coverslips in 24-well plates. After 1 h, complete medium containing 2.5 ng/mL NGF 2.5S (Gibco, Cat# 13257019) was added. Neurons were cultured for 12–24 h prior to electrophysiological recording.

Whole-cell electrophysiology recordings of DRG neurons.

The extracellular solution contained (in mM): 137 mM NaCl, 5 mM KCl, 1 mM $MgCl_2$, 2 mM $CaCl_2$,10 mM HEPES, 10 mM Glucose (pH adjusted to 7.4 with NaOH). The pipette solution contained 133 mM CsCl, 1 mM $MgCl_2$, 1 mM $CaCl_2$, 5 mM EGTA, 4 mM Na_2ATP, 10 mM HEPES (pH adjusted to 7.4 with CsOH).

Patch-clamp recordings were performed at room temperature (22–24 °C). Patch pipettes were pulled from borosilicate glass capillaries (Sutter Instrument, Cat# BF150-86-10) using a P-97 puller (Sutter Instrument) and had a resistance of 2.0–4.0 MΩ. Recordings were acquired using an Axopatch 200B or 700B amplifier (Molecular Devices) and pClamp 11.3 software. Signals were digitized using a Digidata 1550B (Molecular Devices), acquired at a sampling rate of 20 kHz and filtered at 10kHz using the amplifier's low-pass Bessel filter.

Mechanical stimulation of DRG neurons was applied using a heat-polished glass pipette (tip diameter ~3 µm) positioned at a 60° angle to the cover glass surface, controlled by a piezoelectric actuator (K-Cube, KPC101; Thorlabs). Cells were subjected to indentation steps (depth: 4.0 µm + 0.5 µm increments) lasting 300 ms with a 5 s inter-stimulus interval. For pharmacological experiments, CBD was added directly to the bath solution at 10 µM for DRG neurons.

DRG mechanosensitive current analysis

Clampfit 11.2 (Molecular Devices) was used for the analysis of recorded signals and corresponding biophysical parameters. Mechanosensitive current components were characterized by fitting the current traces with a product of exponentials function, defined as:

$$f(t) = \sum_{i=1}^{n} A_i(1 - e^{-t/\tau_{n_i}})(e^{-t/\tau_{d_i}}) + C$$

Based on the decay time constant τ_d obtained from the fitting, the mechanosensitive current components were classified into three types: Rapidly Adapting (RA): $\tau_d < 10$ ms, Intermediate Adapting (IA): 10 ms $\leq \tau_d \leq 30$ ms, Slowly Adapting (SA): $\tau_d > 30$ ms, When multiple exponential components were identified, the relative contribution of each component to the total current amplitude was calculated as follows:

$$\text{Contribution Percentage} = \frac{A_i}{\sum_{i=1}^{n} A_i} \times 100\%$$

Cell lines

The Piezo1-KO-HEK293T cells (the endogenous PIEZO1 is deleted) were either obtained from Ardem Patapoutian lab[46] or generated in this study. We designed specific sgRNAs using Benchling and inserted them into the pSpCas9(BB)-2A-GFP vector (PX458, Addgene, Cat# 48138). After transfecting the HEK293T cell line, EGFP-expressing cells were collected via fluorescence-activated cell sorting (FACS) at the 48-hour mark to enrich for transfected populations. Following a period of expansion to facilitate plasmid clearance, individual EGFP-negative cells were isolated into 96-well plates. Finally, the absence of the PIEZO1 protein in the selected clones was verified by Western blotting. The cells were cultured in Dulbecco's Modified Eagle Medium (Gibco, Cat# 11995-065), supplemented with 10% fetal bovine serum (FBS, Sigma, Cat# F2442) and 1% penicillin/streptomycin (Gibco, Cat# 15-140-122). Cultures were maintained in a 5% CO_2 atmosphere at 37°C.

Transfection

For electrophysiological characterization, cells seeded in 24-well plates were transiently transfected with the appropriate plasmids using polyethylenimine (PEI, Polysciences, Cat# 24314-2). The culture medium was replaced post-transfection, and patch-clamp recordings were performed 24–48 hours after transfection. mPiezo1 and mPiezo2-variant 2 were gift from Ardem Patapoutian lab, while hPIEZO1-variant 2 was a gift from John Wood lab.

Whole-cell electrophysiology of HEK293 cells

The patch-clamp recording protocols using an Axopatch 200B amplifier (Axon Instruments) or HEKA EPC10 were largely consistent with those detailed previously[7]. For whole-cell configuration, borosilicate glass electrodes were polished to a final resistance of 3–6 MΩ when filled with an internal solution containing (in mM): 133 CsCl, 1 $CaCl_2$, 1 $MgCl_2$, 5 EGTA, 10 HEPES, 4 MgATP, and 0.4 Na_2GTP (pH adjusted to 7.3 with CsOH). The extracellular bath solution comprised (in mM): 133 NaCl, 3 KCl, 2.5 $CaCl_2$, 1 $MgCl_2$, 10 HEPES, and 10 glucose (pH adjusted to 7.3 with NaOH). Current signals were sampled at 20 kHz, low-pass filtered at 2 kHz, and acquired using Clampex 10.4 (Axon Instruments). Leak currents, measured prior to mechanical stimulation, were subtracted offline from the evoked traces. Mechanical stimuli were delivered via a fire-polished glass pipette (tip diameter: 3–4 μm) mounted on a piezoelectric driver (E625LVPZT Controller/Amplifier; Physik Instrumente). The probe was positioned adjacent to the cell at an 80° angle and advanced toward the membrane at a velocity of 1 μm/ms during the ramp phase of both approach and retraction. Each mechanical stimulus lasted 150 ms. Stepwise increments of 1 μm were applied at 8 s intervals until patch rupture. Throughout the recording, cells were held at

−80 mV to monitor inward currents. All the experiments were performed at room temperature. In washout experiments, currents were recorded sequentially from the same HEK293T cell in control extracellular solution, followed by perfusion with 10 μM CBD, and finally after washout with CBD-free solution.

Protein expression and purification of PIEZO2

The expression and purification of mPIEZO2 proteins were conducted by following our previously reported procedures[47]. For each batch of protein purification, transfected HEK293T cells cultured in 60 150 × 25-mm Petri dishes with a total of 1.2 L of culture medium were collected by centrifugation at 850 *g* and solubilized in buffer A, containing 25 mM NaPIPES pH 7.3, 150 mM NaCl, 3 mM dithiothreitol (DTT), a mixture of detergents including 0.012% (w/v) GDN, 0.1% (w/v) C12E9, 1% (w/v) CHAPS, 0.5% (w/v) PC, a cocktail of protease inhibitors (MedChemExpress, Cat# HY-K0010) and 3 mM phenylmethylsulfonyl fluoride (PMSF) at 4°C for 3 h. After centrifugation at 13,000 *g* for 30 min, the supernatant was collected and incubated with glutathione sepharose beads (LABLEAD) at 4°C for 6 h. Then the beads were washed 6 times with buffer B, containing 25 mM Na-PIPES pH 7.3, 150 mM NaCl, 3 mM DTT and 0.05% (w/v) GDN. The GST-tagged PIEZO2 was cleaved off by PreScission Protease in buffer B at 4°C for 16 h, and subjected to size-exclusion chromatography (Superpose-6 10/300 GL, GE Healthcare) in FPLC buffer, containing 25 mM Na-PIPES pH 7.3, 150 mM NaCl, 3 mM DTT and 0.02% (w/v) GDN. All detergents used in this project were purchased from Anatrace.

Biolayer Interferometry (BLI) assay

The binding kinetics and affinity between mPIEZO2 proteins and the CBD compound were evaluated using a BLI assay on an Octet R8 system (Sartorius). All experiments were performed at 15°C with a plate shaking speed of 1000 rpm. Briefly, biotinylated target protein (50 μg/mL) was immobilized onto Super Streptavidin (SSA) biosensors (Sartorius) for 1800 seconds. To eliminate bulk refractive index shifts caused by the compound solvent, the running buffer was strictly matched to contain exactly 0.25% DMSO, ensuring identical solvent composition across all sample wells. Following a baseline equilibration step of 60 seconds in the running buffer, the protein-loaded biosensors were dipped into wells containing serial dilutions of CBD (4.69, 9.38, 18.8, 37.5 and 75 μM) for 80 seconds to record the association phase. Subsequently, the biosensors were moved to wells containing only the running buffer for 80 seconds to monitor the dissociation phase. Reference biosensors (loaded with protein but exposed only to running buffer) and reference wells (buffer without compound) were included for double-referencing to subtract non-specific binding and baseline drift. Data processing and kinetic parameter analysis were performed using the Octet Analysis Studio Software (version 13.0), fitting the binding sensorgrams to a 1:1 binding model with global analysis.

Statistics

All statistical analyses for patch-clamp recordings and animal behavior experiments were performed using GraphPad Prism 8.0.2. Single-channel conductance, all-points histogram fitting and inactivation kinetics of DRG currents were fitted using Clampfit 11.3. Data are presented as mean ± SEM, with individual data points overlaid where

applicable. The sample size (n) refers to the number of cells recorded and is indicated in the corresponding figure legends. All experiments were biologically independent. Differences between groups were assessed using Student's t-test, two-way ANOVA, or Chi-square test. Significance levels are denoted as follows: ns, $P > 0.05$; *$P < 0.05$; **$P < 0.01$; ***$P < 0.001$; ****$P < 0.0001$.

Acknowledgments

We thank Dr. Huanghe Yang at Duke University for helpful discussion and the Center of Pharmaceutical Technology and the Laboratory Animal Resources Center at Tsinghua University for technical support. This work was supported by Shenzhen Medical Research Fund B2502023, the National Natural Science Foundation of China grant 32300603, and Guangdong Pearl River Program 2023QN10Y164 to Y.Z., grant numbers 32425003, 2021ZD0203301, 32130049, 32021002, 31825014 from either the National Natural Science Foundation of China or the National Key R&D Program of China, the Beijing Outstanding Young Scientist Program grant, the Fundamental and Interdisciplinary Disciplines Breakthrough Plan of the Ministry of Education of China (JYB2025XDXM601), the New Cornerstone Investigator Program, and the Shenzhen Medical Research Fund (SMRF, B2302016) to B.X.

Author Contributions

Q.H. tested CBD properties, and conducted PIEZO2 protein purification and binding experiments and data analysis; R.L. and H.Z. conducted electrophysiology and data analysis; W.H. and K.C. performed behavioural assays and data analysis; F.Q. provided reagents; Y.Z. and B.X. conceived and directed the study, analyzed data, made figures and wrote the manuscript with help from all other authors.

Competing interests

The authors declare no competing interests.

Author Information

Correspondence and requests for materials should be addressed to Y.Z. (zhangyang@szbl.ac.cn) and B.X. (xbailong@mail.tsinghua.edu.cn).

Data Availability

The data are available upon request from the lead contact.

Figures and Legends

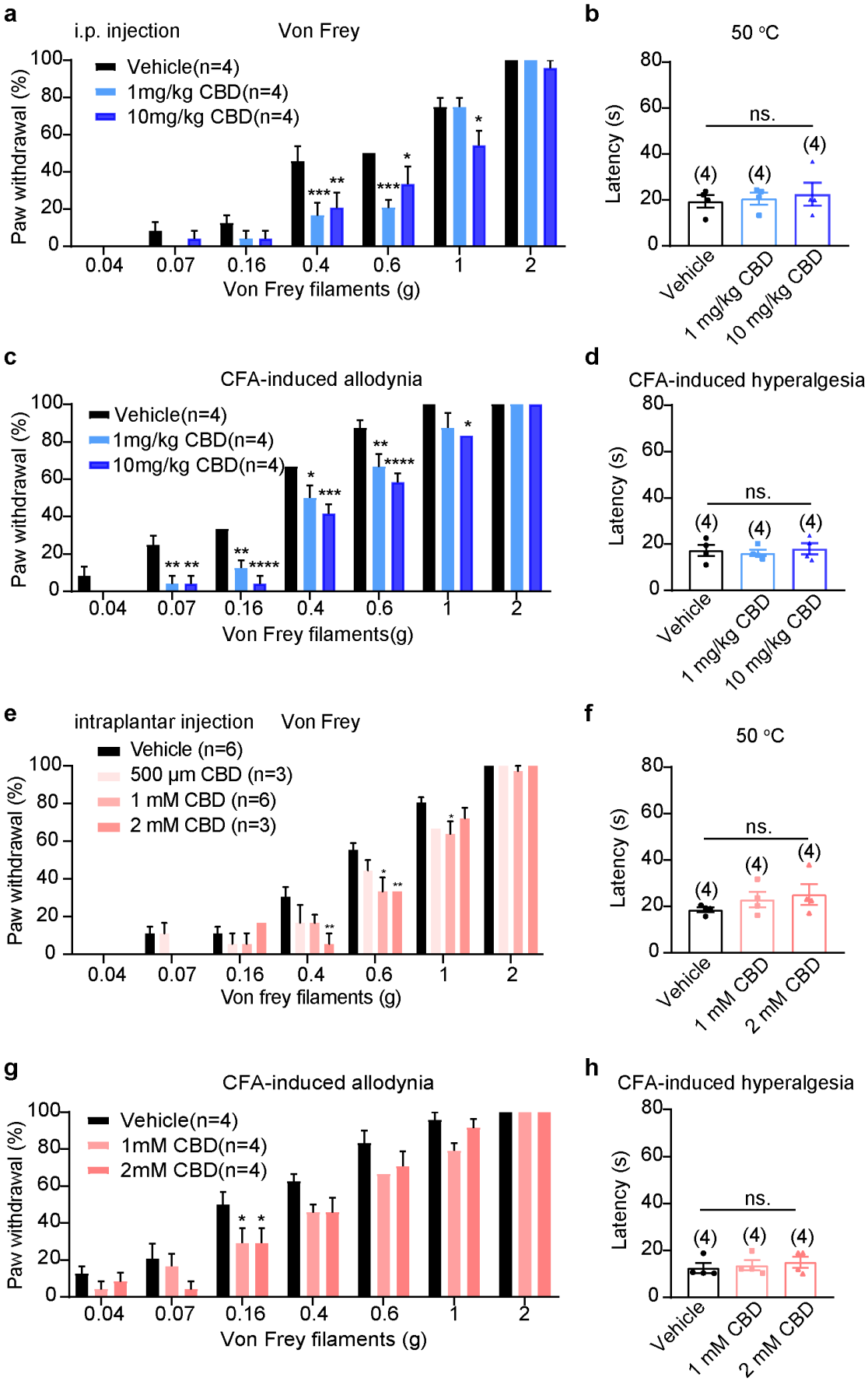

Figure 1. Dose-dependent inhibition of touch and CFA-induced mechanical allodynia by CBD.

(**a**, **c**, **e**, **g**) The percentage of paw withdrawals in response to the indicated series of Von Frey filament stimulation following intraperitoneal injection (**a**, **c**) or intraplantar injection (**e**, **g**) of vehicle or CBD in naive state (**a**, **e**) and CFA-induced pain model (**c**, **g**). Data are mean ± SEM. *$P < 0.05$, **$P < 0.01$, ***$P < 0.001$, ****$P < 0.0001$ (two-way ANOVA). (**b**, **d**, **f**, **h**) Scatterplot of the paw withdrawal latency in response to the hot plate test intraperitoneal injection (**b**, **d**) or intraplantar injection (**f**, **h**) vehicle or CBD in naive states (**b**, **f**) and CFA-induced pain model (**d**, **h**). Data are mean ± SEM (one-way ANOVA).

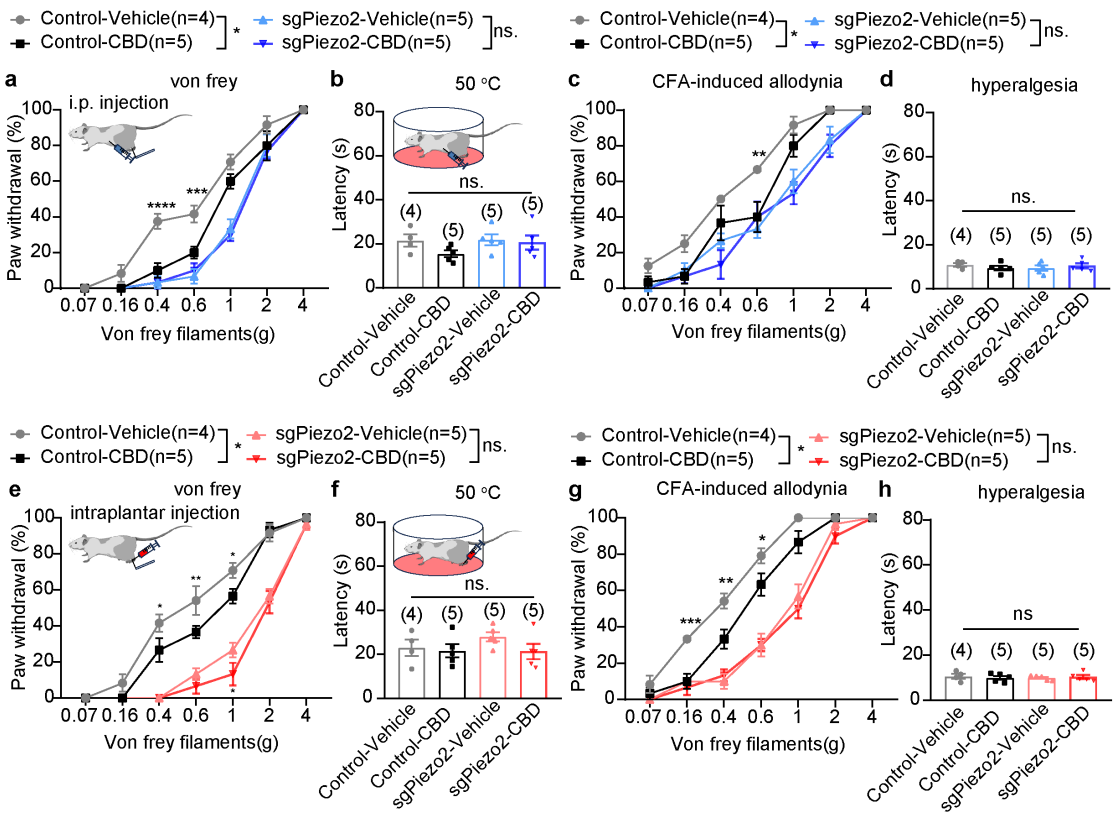

Figure 2. Piezo2 dependency of CBD-induced inhibition of touch and mechanical allodynia in mice.

(**a-d**) Behavioral assessment of the control and sgPiezo2-targeted mice following intraperitoneal injection of vehicle or CBD in either naïve state (**a**, **b**) or CFA-induced inflammatory pain model (**c**, **d**). **a**, **c**, The percentage of paw withdrawals in response to the indicated series of Von Frey filament stimulation in naïve state (**a**) or CFA-induced pain model (**c**). **b**, **d,** Scatterplots of the latency in response to the hot plate test in naïve state (**b**) or CFA-induced pain model (**d**). Groups: Control (vehicle, n=4 mice; 10mg/kg CBD, n=5 mice); sgPiezo2 (vehicle, n=5 mice; 10mg/kg CBD, n=5 mice). Data are mean ± SEM. **P* < 0.05, ***P* < 0.01, ****P* < 0.001, *****P* < 0.0001 (two-way ANOVA for **a** and **c**; one-way ANOVA for **b** and **d**).

(**e-h**) Behavioral assessment of the control and sgPiezo2-targeted mice following intraplantar injection of vehicle or CBD in either naïve state (**e**, **f**) or CFA-induced inflammatory pain model (**g**, **h**). **e**, **g**, The percentage of paw withdrawals in response to the indicated series of Von Frey filament stimulation in naïve state (**e**) or CFA-induced pain model (**g**). **f**, **h**, Scatterplots of the latency in response to the hot plate test in naïve state (**f**) or CFA-induced pain model (**h**). Groups: Control (vehicle, n=4 mice; 2mM CBD, n=5 mice); sgPiezo2 (vehicle, n=5 mice; 2mM CBD, n=5 mice). Data are mean ± SEM. **P* < 0.05, ***P* < 0.01, ****P* < 0.001 (two-way ANOVA for **e** and **g**; one-way ANOVA for **f** and **h**).

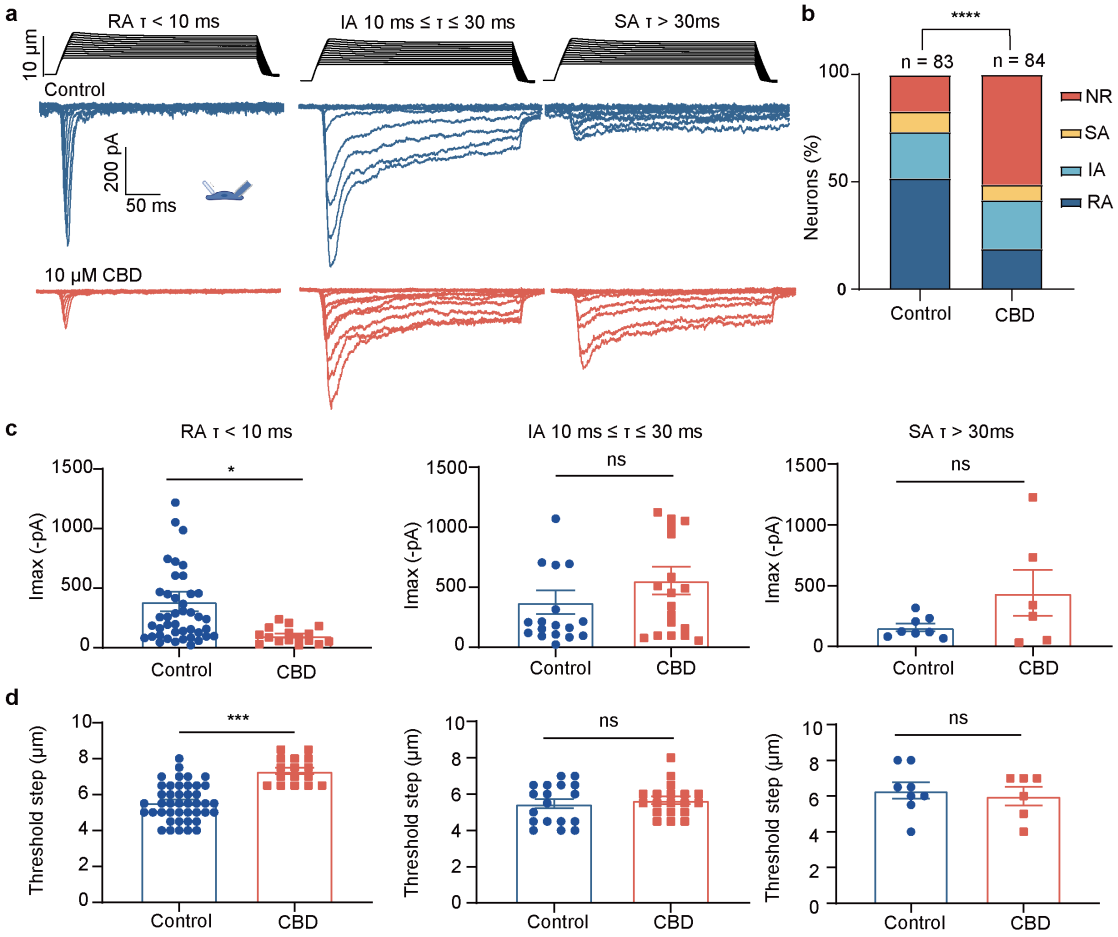

Figure 3. CBD selectively suppresses rapidly adapting mechanosensitive currents in DRG neurons.

(a) Representative mechanosensitive currents from vehicle control or 10 µM CBD-treated DRG neurons, displaying rapidly adapting (RA), intermediately adapting (IA), and slowly adapting (SA) phenotypes. **(b)** Proportions of RA, IA, SA, and non-responding (NR) neurons in control (n = 83) and CBD-treated (n = 84) groups. ****P < 0.0001(Chi-squared test). **(c)** Peak current amplitudes (I_{max}) in RA, IA, and SA neurons. CBD significantly reduced I_{max} in RA neurons (Control, n = 43, CBD, n = 16; *P <0.05) but had no significant effect on IA or SA neurons (ns). **(d)** Mechanical activation thresholds in RA, IA, and SA neurons. CBD increased the activation threshold in RA neurons (Control, n = 43, CBD, n = 16; ****P < 0.0001) without affecting IA or SA neurons (ns). Data are mean ± SEM. Statistical significance determined by a two-tailed unpaired Student's t-test.

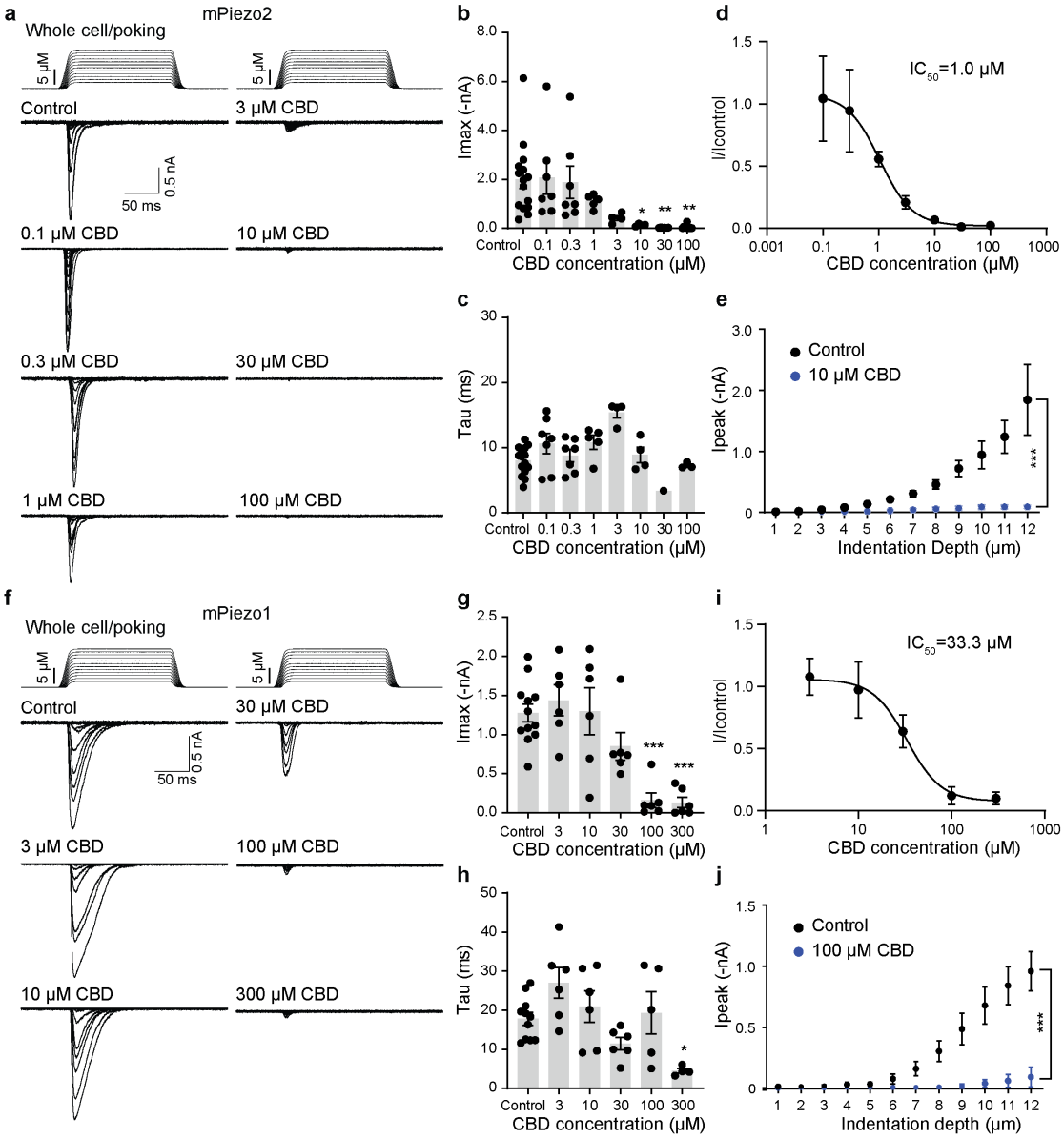

Figure 4. Selective inhibition of mPiezo2 over mPiezo1 by CBD

(**a**) Representative traces of poking-induced inward currents recorded at -80 mV in mPiezo2-expressing Piezo1-KO-HEK293T cells treated with 0.1-100 μM CBD for 10 minutes. (**b**, **c**) Scatter plots of maximum poking-induced current amplitude (**b**) and inactivation Tau (**c**) of mPiezo2-mediated currents following treatment with various concentrations of CBD. one-way ANOVA followed by post Dunnett test, *$P < 0.05$, **$P < 0.01$, ***$P < 0.001$, ****$P < 0.0001$. (**d**) Concentration–response curve of the inhibitory effect of CBD on mPiezo2 current. Whole-cell currents were normalized to the vehicle control group. The solid line shows the fit to a four-parameter Hill equation (IC_{50} = 1.0 μM). Data points represent mean ± SEM. (**e**) Poking step-current relationship curves of mPiezo2 in the absence (vehicle control) or presence of 10 μM CBD. Data are shown as mean ± SEM. ***$P < 0.001$ (two-way ANOVA). (**f**) Representative traces of poking-induced inward currents recorded at -80 mV in mPiezo1-expressing Piezo1-KO-HEK293T cells treated with 3-300 μM CBD for 10 minutes. (**g**, **h**) Scatter plots of maximum poking-induced current amplitude (**g**) and

inactivation Tau (**h**) of mPiezo1-mediated currents following treatment with various concentrations of CBD. one-way ANOVA followed by post Dunnett test, $*P < 0.05$, $**P < 0.01$, $***P < 0.001$, $****P < 0.0001$. (**i**) Concentration–response curve of the inhibitory effect of CBD on mPiezo1 current. Whole-cell currents were normalized to the control group. The solid line shows the fit to a four-parameter Hill equation (IC_{50} = 33.3 μM). Data points represent mean ± SEM. (**j**) Poking step-current relationship curves of mPiezo1 in the absence (vehicle control) or presence of 100 μM CBD. Data are shown as mean ± SEM. $***P < 0.001$ (two-way ANOVA).

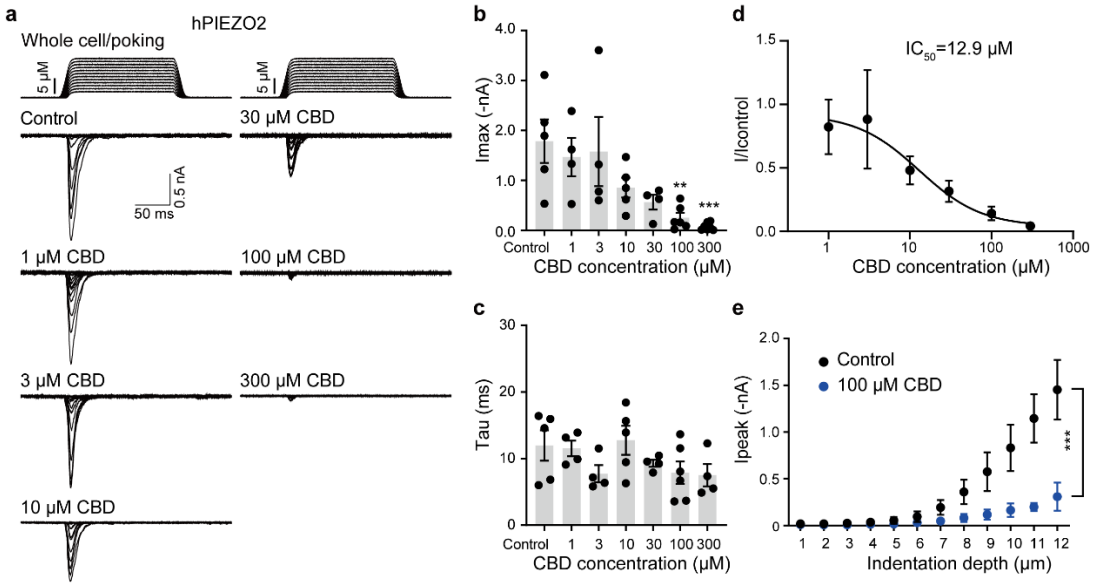

Figure 5. CBD inhibition of the mechanically activated currents mediated by the hPIEZO2

(**a**) Representative traces of poking-induced inward currents recorded at -80 mV in hPIEZO2-expressing Piezo1-KO-HEK293T cells treated with 1-300 μM CBD for 10 minutes. (**b**, **c**) Scatter plots of maximum poking-induced current amplitude (**b**) and inactivation Tau (**c**) of hPIEZO2-mediated currents following treatment with various concentrations of CBD. one-way ANOVA followed by post Dunnett test, *$P < 0.05$, **$P < 0.01$, ***$P < 0.001$, ****$P < 0.0001$. (**d**) Concentration–response curve of the inhibitory effect of CBD on hPIEZO2 current. Whole-cell currents were normalized to the control group. The solid line shows the fit to a four-parameter Hill equation (IC_{50} = 12.9 μM). Data points represent mean ± SEM. (**e**) Poking step-current relationship curves of hPIEZO2 in the absence (vehicle control) or presence of 100 μM CBD. Data are shown as mean ± SEM. ***$P < 0.001$ (two-way ANOVA).

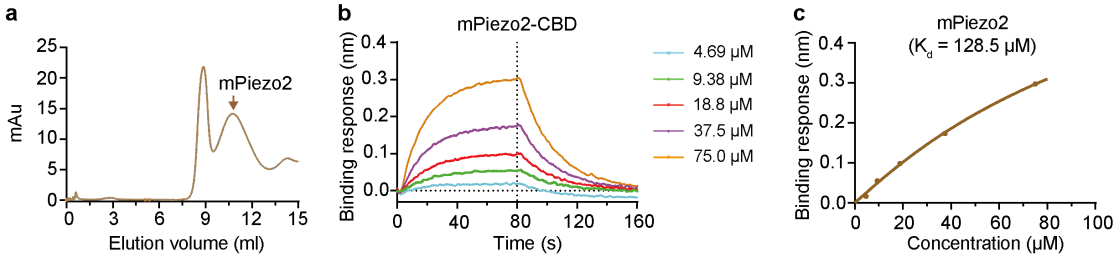

Figure 6. CBD dose-dependent binding to purified mPiezo2 proteins

(**a**) Representative FPLC profiles of purified mPiezo2 proteins.

(**b**) Representative binding traces of the indicated doses of CBD to purified mPiezo2 proteins. The horizontal dashed line indicates the baseline, while the vertical dashed line indicates the start of compound wash-off.

(**c**) Dose-binding curves of CBD and mPiezo2 fitted with a Hill equation. The estimated dissociation constant (K_d) values are labeled.

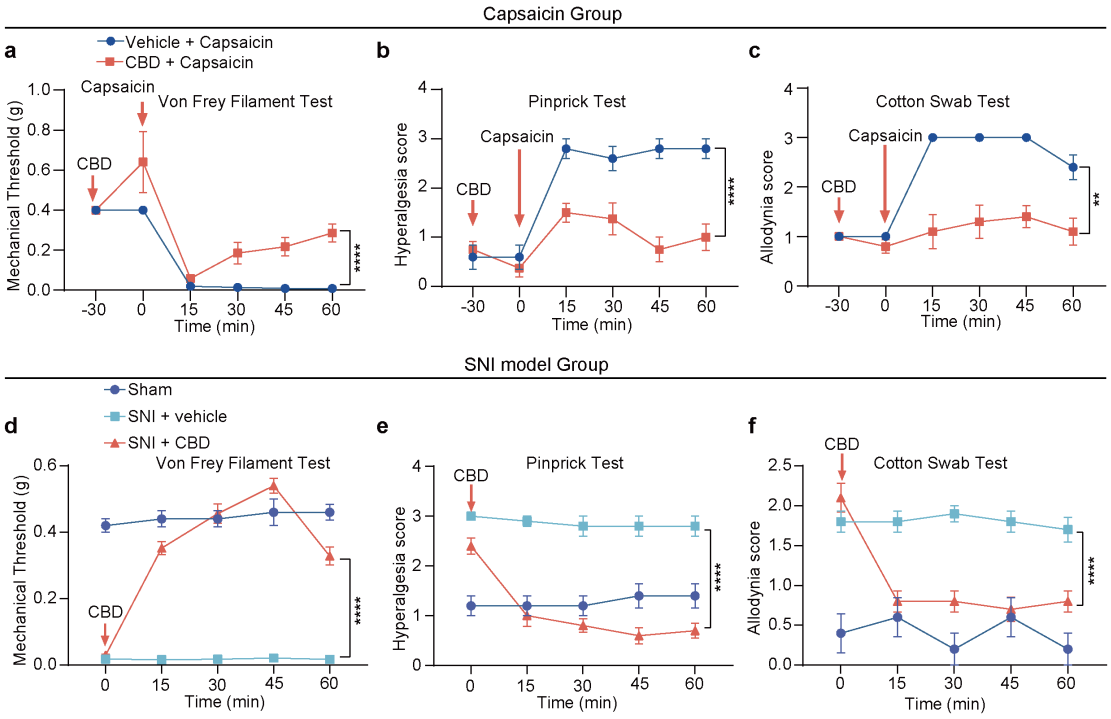

Extended Data Figure 1. CBD attenuates mechanical allodynia across acute, inflammatory, and neuropathic pain models.

(**a–c**) Behavioral assessment of mechanical sensitivity in the capsaicin-induced pain model. **a**, Time course of mechanical thresholds assessed by von Frey filaments. **b**, **c**, Mechanical hyperalgesia and allodynia scores assessed by pinprick (**b**) and cotton swab (**c**) tests. Groups: Capsaicin (1 μg, vehicle; $n = 5$ mice); Capsaicin + CBD (1 μg, 20 mg kg^{-1} CBD; $n = 10$ mice). Data are mean ± SEM. $^{**}P < 0.01$, $^{****}P < 0.0001$ (two-way ANOVA). (**d–f**) Assessment of mechanical sensitivity in the spared nerve injury (SNI) model. **d**, Time course of mechanical thresholds (von Frey). **e**, **f**, Mechanical hyperalgesia and allodynia scores assessed by pinprick (**e**) and cotton swab (**f**) tests. Groups: Sham ($n = 5$ mice); SNI (vehicle; $n = 10$ mice); SNI + CBD (20 mg kg^{-1} CBD; $n = 10$ mice). Data are mean ± SEM. $^{****}P < 0.0001$ (two-way ANOVA).

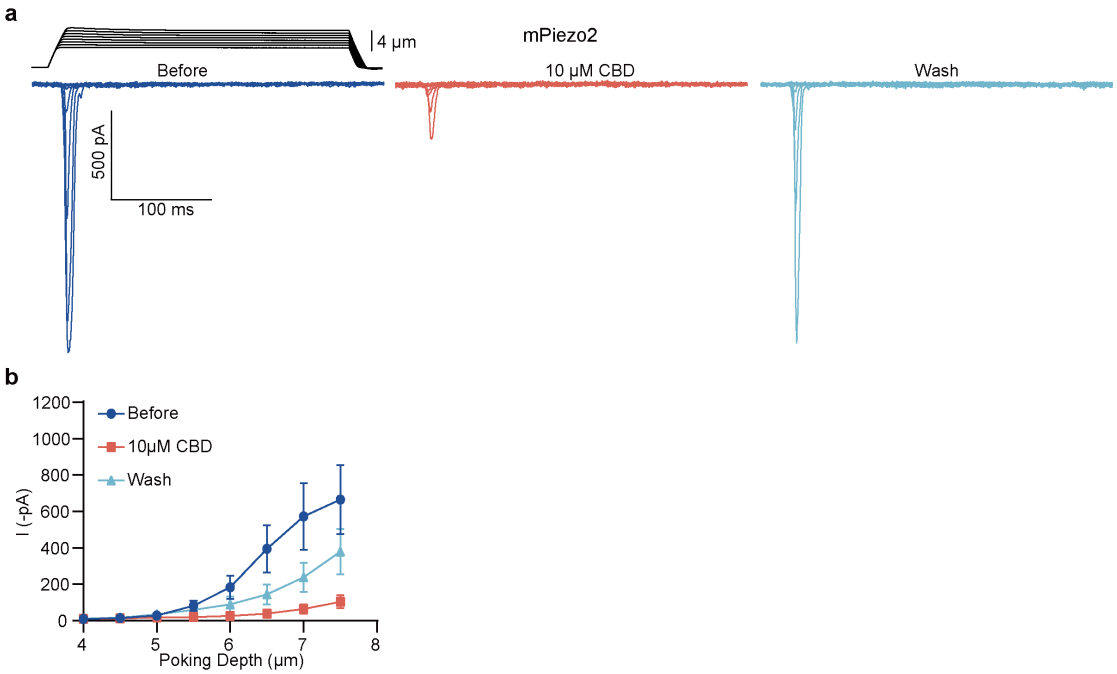

Extended Data Figure 2. CBD reversibly inhibits mPiezo2-mediated mechanically activated currents.

(a) Representative whole-cell currents in mPiezo2-expressing cells evoked by mechanical indentation recorded before, during application of 10 μM CBD, and after washout. **(b)** Stimulus-response relationships of currents evoked by increasing displacement depths as shown in **a**. Data are mean ± SEM (n = 10).

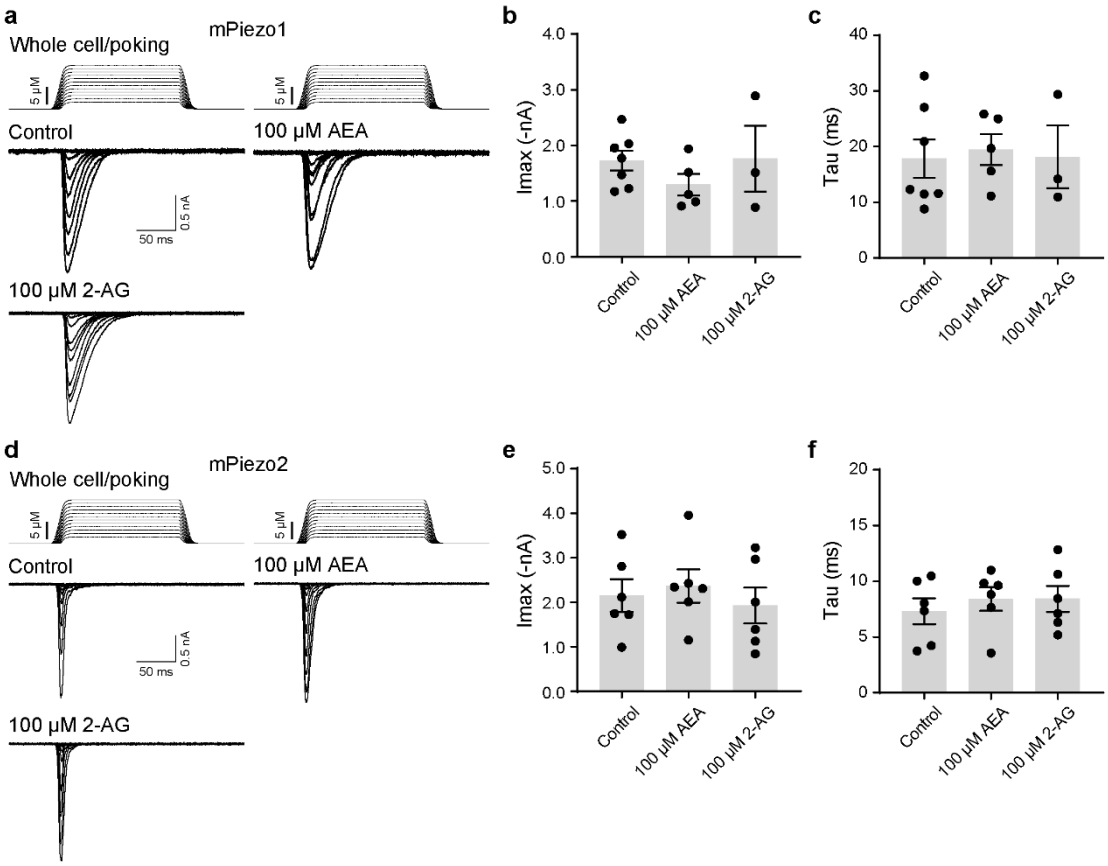

Extended Data Figure 3. mPiezo1/2-mediated currents are insensitive to activation of canonical cannabinoid receptors.

(a, d) Representative whole-cell mPiezo1 (**a**) or mPiezo2 (**d**) currents evoked by mechanical stimulation in the absence or presence of the indicated cannabinoid receptor agonist AEA or 2-AG. **(b, e)** Maximal current amplitudes of mPiezo1 (**b**) or mPiezo2 (**e**) under the indicated treatment conditions. (**c, f**) Scatter plot of the inactivation tau of mPiezo1- (**c**) or mPiezo2- (**f**) mediated currents under the indicated treatment conditions. Data are mean ± SEM (one-way ANOVA).

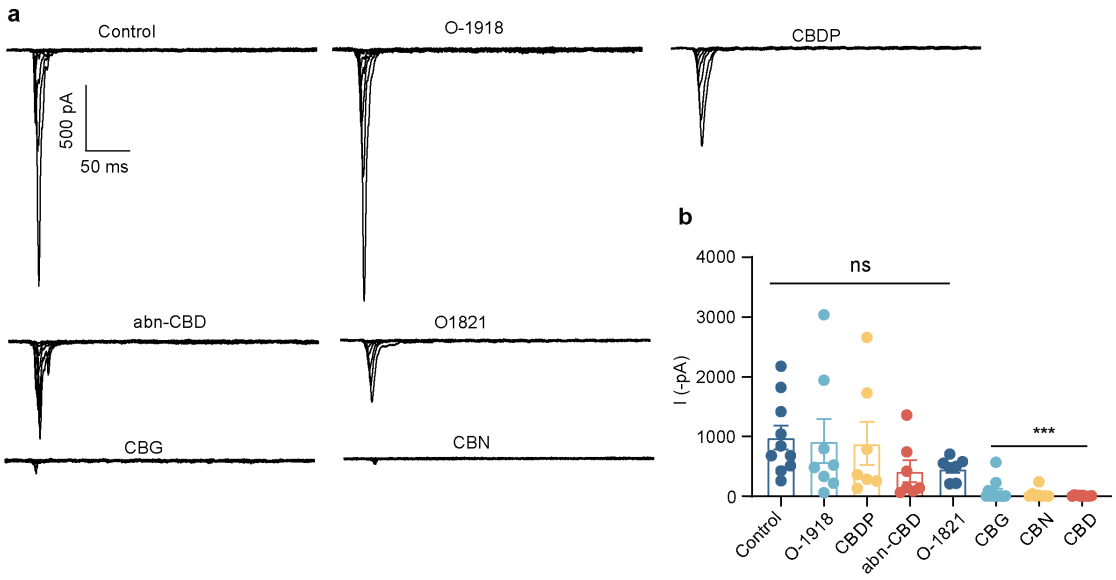

Extended Data Figure 4. CBD analogs differentially modulate mPiezo2-mediated currents.

(a) Representative whole-cell mPiezo2 currents evoked by mechanical stimulation in the presence of the indicated compounds. **(b)** Maximal current amplitudes across all groups. CBD (n = 10), CBG (n = 12), and CBN (n = 8) significantly suppressed mPiezo2 currents (***$P < 0.001$), while O1821 (n = 7), abn-CBD (n = 7) O-1918 (n = 8) and CBDP (n = 7) showed no significant effect (ns). Data are mean ± SEM. Unpaired Student's t-test.

Reference

1 Pacher, P., Kogan, N. M. & Mechoulam, R. Beyond THC and Endocannabinoids. *Annual review of pharmacology and toxicology* **60**, 637-659, doi:10.1146/annurev-pharmtox-010818-021441 (2020).

2 Kalaba, M. & Ware, M. A. Cannabinoid Profiles in Medical Cannabis Users: Effects of Age, Gender, Symptoms, and Duration of Use. *Cannabis Cannabinoid Res* **7**, 840-851, doi:10.1089/can.2020.0120 (2022).

3 Britch, S. C., Babalonis, S. & Walsh, S. L. Cannabidiol: pharmacology and therapeutic targets. *Psychopharmacology (Berl)* **238**, 9-28, doi:10.1007/s00213-020-05712-8 (2021).

4 Henderson, L. A. *et al.* Medicinal cannabis in the treatment of chronic pain. *Aust J Gen Pract* **50**, 724-732, doi:10.31128/AJGP-04-21-5939 (2021).

5 Harris, H. M. *et al.* Delta-9-tetrahydrocannabinol and Cannabidiol for Pain: Preclinical and Clinical Models. *Curr Top Behav Neurosci* **76**, 389-431, doi:10.1007/7854_2025_604 (2026).

6 Cortez-Resendiz, A. *et al.* The Pharmacology of Cannabinoids in Chronic Pain. *Med Cannabis Cannabinoids* **8**, 31-46, doi:10.1159/000543813 (2025).

7 Coste, B. *et al.* Piezo1 and Piezo2 are essential components of distinct mechanically activated cation channels. *Science* **330**, 55-60, doi:10.1126/science.1193270 (2010).

8 Ranade, S. S. *et al.* Piezo2 is the major transducer of mechanical forces for touch sensation in mice. *Nature* **516**, 121-125, doi:10.1038/nature13980 (2014).

9 Murthy, S. E. *et al.* The mechanosensitive ion channel Piezo2 mediates sensitivity to mechanical pain in mice. *Science translational medicine* **10**, doi:10.1126/scitranslmed.aat9897 (2018).

10 Chesler, A. T. *et al.* The Role of PIEZO2 in Human Mechanosensation. *The New England journal of medicine*, doi:10.1056/NEJMoa1602812 (2016).

11 Szczot, M. *et al.* PIEZO2 mediates injury-induced tactile pain in mice and humans. *Science translational medicine* **10**, doi:10.1126/scitranslmed.aat9892 (2018).

12 Devinsky, O., Cross, J. H. & Wright, S. Trial of Cannabidiol for Drug-Resistant Seizures in the Dravet Syndrome. *The New England journal of medicine* **377**, 699-700, doi:10.1056/NEJMc1708349 (2017).

13 Thiele, E. A. *et al.* Cannabidiol in patients with seizures associated with Lennox-Gastaut syndrome (GWPCARE4): a randomised, double-blind, placebo-controlled phase 3 trial. *Lancet* **391**, 1085-1096, doi:10.1016/S0140-6736(18)30136-3 (2018).

14 Mechoulam, R. A Delightful Trip Along the Pathway of Cannabinoid and Endocannabinoid Chemistry and Pharmacology. *Annual review of pharmacology and toxicology* **63**, 1-13, doi:10.1146/annurev-pharmtox-051921-083709 (2023).

15 Gulbransen, G., Xu, W. & Arroll, B. Cannabidiol prescription in clinical practice: an audit on the first 400 patients in New Zealand. *BJGP Open* **4**, doi:10.3399/bjgpopen20X101010 (2020).

16 McPartland, J. M., Duncan, M., Di Marzo, V. & Pertwee, R. G. Are cannabidiol and Delta(9)-tetrahydrocannabivarin negative modulators of the endocannabinoid system? A systematic review. *British journal of pharmacology* **172**, 737-753, doi:10.1111/bph.12944 (2015).

17 Pertwee, R. G. Pharmacology of cannabinoid CB1 and CB2 receptors. *Pharmacol Ther* **74**,

129-180, doi:10.1016/s0163-7258(97)82001-3 (1997).

18 Navarro, G. *et al.* Cannabidiol skews biased agonism at cannabinoid CB(1) and CB(2) receptors with smaller effect in CB(1)-CB(2) heteroreceptor complexes. *Biochem Pharmacol* **157**, 148-158, doi:10.1016/j.bcp.2018.08.046 (2018).

19 Costa, B., Trovato, A. E., Comelli, F., Giagnoni, G. & Colleoni, M. The non-psychoactive cannabis constituent cannabidiol is an orally effective therapeutic agent in rat chronic inflammatory and neuropathic pain. *Eur J Pharmacol* **556**, 75-83, doi:10.1016/j.ejphar.2006.11.006 (2007).

20 Bisogno, T. *et al.* Molecular targets for cannabidiol and its synthetic analogues: effect on vanilloid VR1 receptors and on the cellular uptake and enzymatic hydrolysis of anandamide. *British journal of pharmacology* **134**, 845-852, doi:10.1038/sj.bjp.0704327 (2001).

21 Qin, N. *et al.* TRPV2 is activated by cannabidiol and mediates CGRP release in cultured rat dorsal root ganglion neurons. *The Journal of neuroscience : the official journal of the Society for Neuroscience* **28**, 6231-6238, doi:10.1523/JNEUROSCI.0504-08.2008 (2008).

22 De Petrocellis, L. *et al.* Plant-derived cannabinoids modulate the activity of transient receptor potential channels of ankyrin type-1 and melastatin type-8. *J Pharmacol Exp Ther* **325**, 1007-1015, doi:10.1124/jpet.107.134809 (2008).

23 Etemad, L., Karimi, G., Alavi, M. S. & Roohbakhsh, A. Pharmacological effects of cannabidiol by transient receptor potential channels. *Life Sci* **300**, 120582, doi:10.1016/j.lfs.2022.120582 (2022).

24 Julius, D. TRP channels and pain. *Annual review of cell and developmental biology* **29**, 355-384, doi:10.1146/annurev-cellbio-101011-155833 (2013).

25 Britch, S. C., Goodman, A. G., Wiley, J. L., Pondelick, A. M. & Craft, R. M. Antinociceptive and Immune Effects of Delta-9-Tetrahydrocannabinol or Cannabidiol in Male Versus Female Rats with Persistent Inflammatory Pain. *J Pharmacol Exp Ther* **373**, 416-428, doi:10.1124/jpet.119.263319 (2020).

26 Feng, J., Page, J., Chung, L., He, Z. & Wang, K. H. Rapid suppression of neuropathic pain and somatosensory hyperactivity by nano-formulated cannabidiol. *Cell Chem Biol* **32**, 1412-1428 e1415, doi:10.1016/j.chembiol.2025.10.005 (2025).

27 Abraham, A. D. *et al.* Orally consumed cannabinoids provide long-lasting relief of allodynia in a mouse model of chronic neuropathic pain. *Neuropsychopharmacology* **45**, 1105-1114, doi:10.1038/s41386-019-0585-3 (2020).

28 Xiao, B. Mechanisms of mechanotransduction and physiological roles of PIEZO channels. *Nature reviews. Molecular cell biology* **25**, 886-903, doi:10.1038/s41580-024-00773-5 (2024).

29 Szczot, M., Nickolls, A. R., Lam, R. M. & Chesler, A. T. The Form and Function of PIEZO2. *Annu Rev Biochem* **90**, 507-534, doi:10.1146/annurev-biochem-081720-023244 (2021).

30 Murthy, S. E., Dubin, A. E. & Patapoutian, A. Piezos thrive under pressure: mechanically activated ion channels in health and disease. *Nature reviews. Molecular cell biology* **18**, 771-783, doi:10.1038/nrm.2017.92 (2017).

31 Woo, S. H. *et al.* Piezo2 is required for Merkel-cell mechanotransduction. *Nature*, doi:10.1038/nature13251 (2014).

32 Xie, Z. *et al.* Piezo2 channels expressed by colon-innervating TRPV1-lineage neurons

mediate visceral mechanical hypersensitivity. *Neuron* **111**, 526-538 e524, doi:10.1016/j.neuron.2022.11.015 (2023).

33 Obeidat, A. M. *et al.* Piezo2 expressing nociceptors mediate mechanical sensitization in experimental osteoarthritis. *Nature communications* **14**, 2479, doi:10.1038/s41467-023-38241-x (2023).

34 Adamczyk, N. S. *et al.* FM-dye inhibition of Piezo2 relieves acute inflammatory and osteoarthritis knee pain in mice of both sexes. *bioRxiv*, doi:10.1101/2025.03.17.643683 (2025).

35 Alcaino, C., Knutson, K., Gottlieb, P. A., Farrugia, G. & Beyder, A. Mechanosensitive ion channel Piezo2 is inhibited by D-GsMTx4. *Channels* **11**, 245-253, doi:10.1080/19336950.2017.1279370 (2017).

36 Bae, C., Sachs, F. & Gottlieb, P. A. The mechanosensitive ion channel Piezo1 is inhibited by the peptide GsMTx4. *Biochemistry* **50**, 6295-6300, doi:10.1021/bi200770q (2011).

37 Zhang, M., Wang, Y., Geng, J., Zhou, S. & Xiao, B. Mechanically Activated Piezo Channels Mediate Touch and Suppress Acute Mechanical Pain Response in Mice. *Cell reports* **26**, 1419-1431 e1414, doi:10.1016/j.celrep.2019.01.056 (2019).

38 Sofia, R. D., Vassar, H. B. & Knobloch, L. C. Comparative analgesic activity of various naturally occurring cannabinoids in mice and rats. *Psychopharmacologia* **40**, 285-295, doi:10.1007/BF00421466 (1975).

39 Moore, C. F. & Weerts, E. M. Cannabinoid tetrad effects of oral Delta9-tetrahydrocannabinol (THC) and cannabidiol (CBD) in male and female rats: sex, dose-effects and time course evaluations. *Psychopharmacology (Berl)* **239**, 1397-1408, doi:10.1007/s00213-021-05995-5 (2022).

40 Arantes, A. L. F. *et al.* Antinociceptive action of cannabidiol on thermal sensitivity and post-operative pain in male and female rats. *Behav Brain Res* **459**, 114793, doi:10.1016/j.bbr.2023.114793 (2024).

41 Jiang Yan, W. H., Hailong Yao, Yan Chen, Cheng Bi, Tianyuan Ye, Shangkun Wang, Hongda Yin, Bailong Xiao. Mouse behavioral genomics identifies Creld1 as a gatekeeper of somatosensation. *bioRxiv*, doi:https://doi.org/10.64898/2026.03.30.715210 (2026).

42 Pengfei Liang, Y.-C. S. W., Ke Zoe Shan, Yang Zhang, Martha Delahunty, Sanjay Khandelwal, Gowthami M. Arepally, Marilyn J. Telen, Huanghe Yang. Cannabidiol Inhibits PIEZO Channels to Mitigate Red Blood Disorders. *bioRxiv*, doi:https://doi.org/10.64898/2026.01.22.700543 (2026).

43 Cao, K., Lai, R., Sun, K., He, Q., Cai, M., Huang, J., Gao, L., Xiao, B., & Zhang, Y. Cannabidiol modulates PIEZO1 activity to regulate uterine contractility and pregnancy outcome. *LangTaoSha Preprint*, doi:https://doi.org/10.65215/LTSpreprints.2026.04.20.000194 (2026).

44 Bourquin, A. F. *et al.* Assessment and analysis of mechanical allodynia-like behavior induced by spared nerve injury (SNI) in the mouse. *Pain* **122**, 14 e11-14, doi:10.1016/j.pain.2005.10.036 (2006).

45 Borbiro, I., Badheka, D. & Rohacs, T. Activation of TRPV1 channels inhibits mechanosensitive Piezo channel activity by depleting membrane phosphoinositides. *Science signaling* **8**, ra15, doi:10.1126/scisignal.2005667 (2015).

46 Syeda, R. *et al.* Chemical activation of the mechanotransduction channel Piezo1. *eLife* **4**,

doi:10.7554/eLife.07369 (2015).

47 Wang, L. *et al.* Structure and mechanogating of the mammalian tactile channel PIEZO2. *Nature* **573**, 225-229, doi:10.1038/s41586-019-1505-8 (2019).